Chemistry and Physics of Lipids 180 (2014) 15–22

Contents lists available at ScienceDirect

Chemistry and Physics of Lipids

journal homepage: www.elsevier.com/locate/chemphyslip

Differential spontaneous folding of mycolic acids from *Mycobacterium tuberculosis*

Wilma Groenewald[a,b], Mark S. Baird[b], Jan A. Verschoor[a], David E. Minnikin[c], Anna K. Croft[b,d,*]

[a] Department of Biochemistry, University of Pretoria, Pretoria 0002, South Africa
[b] School of Chemistry, University of Wales Bangor, Bangor LL57 2UW, UK
[c] Institute of Microbiology and Infection, School of Biosciences, University of Birmingham, Edgbaston, Birmingham B15 2TT, UK
[d] Department of Chemical and Environmental Engineering, University of Nottingham, University Park, Nottingham NG7 2RD, UK

ARTICLE INFO

Article history:
Received 17 September 2013
Received in revised form 6 December 2013
Accepted 9 December 2013
Available online 18 December 2013

Keywords:
Mycolic acid
Mycobacterium tuberculosis
Molecular dynamics
Folding
Principle component analysis

ABSTRACT

Mycolic acids are structural components of the mycobacterial cell wall that have been implicated in the pathogenicity and drug resistance of certain mycobacterial species. They also offer potential in areas such as rapid serodiagnosis of human and animal tuberculosis. It is increasingly recognized that conformational behavior of mycolic acids is very important in understanding all aspects of their function. Atomistic molecular dynamics simulations, *in vacuo*, of stereochemically defined *Mycobacterium tuberculosis* mycolic acids show that they fold spontaneously into reproducible conformational groupings. One of the three characteristic mycolate types, the keto-mycolic acids, behaves very differently from either α-mycolic acids or methoxy-mycolic acids, suggesting a distinct biological role. However, subtle conformational behavioral differences between all the three mycolic acid types indicate that cooperative interplay of individual mycolic acids may be important in the biophysical properties of the mycobacterial cell envelope and therefore in pathogenicity.

© 2013 The Authors. Published by Elsevier Ireland Ltd. Open access under CC BY-NC-ND license.

1. Introduction

Tuberculosis (TB) is the most frequent cause of death in individuals infected with human immunodeficiency virus (HIV), especially in Sub-Saharan Africa. *Mycobacterium tuberculosis*, the causative agent of TB, has a cell wall that is exceptionally rich in lipids, of which mycolic acids (MAs) are the major components (Minnikin, 1982; Minnikin et al., 2002).

MAs are high molecular weight 2-alkyl-3-hydroxy fatty acids, principally covalently bound to arabinogalactan in the cell wall. They are also found as trehalose mono- and- dimycolates (Minnikin et al., 2002; Verschoor et al., 2012) and as free hydroxy acids. MAs from *M. tuberculosis* are found in three main classes, α- (**1**), methoxy- (**2**) and keto-MA (**3**), whose main components are shown in Fig. 1. The methoxy- and keto-MAs both have subclasses, characterized by the presence of *cis*-cyclopropane rings or *trans*-cyclopropane groups with an adjacent methyl branch, the former predominating in methoxy-MAs (**2**) and the latter in keto-MAs (**3**) (Watanabe et al., 2001, 2002). The specified absolute stereochemistries of these mycolic acids have been probed by total syntheses and comparison with natural material (Al Dulayymi et al., 2003, 2005, 2006a,b, 2007; Koza and Baird, 2007; Verschoor et al., 2012).

These and other MA types are present in varying proportions in different species of mycobacteria, affording each a specific MA profile, which can be used to differentiate subspecies of these bacteria (Minnikin and Goodfellow, 1980; Butler and Guthertz, 2001; Song et al., 2009). The existence of specific MA profiles in different contexts (Yuan et al., 1998) suggests that the physical properties of, and thus the biological roles of, both MA derivatives and free MAs may be directed by their underlying chemical make-up. This premise is supported by various studies on the genes that encode for the enzymes involved in synthesising the different MA-functional groups that have highlighted the importance of the different functionalities present in the mycobacteria. Lacking a proximal *cis*-cyclopropane group in α-MA, *M. bovis BCG* mutants were not able to establish a lethal infection, in comparison with the wild type (Glickman et al., 2000). *Trans*-cyclopropanation of oxygenated MAs suppressed *M. tuberculosis*-induced inflammation and virulence (Rao et al., 2006). Cyclopropanation and cyclopropane stereochemistry are, therefore, not to be overlooked in the importance of MA

* Corresponding author at: Department of Chemical and Environmental Engineering, University of Nottingham, University Park, Nottingham, NG7 2RD, UK. Tel.: +44 115 8466391.
E-mail address: anna.croft@nottingham.ac.uk (A.K. Croft).

0009-3084 © 2013 The Authors. Published by Elsevier Ireland Ltd. Open access under CC BY-NC-ND license.
http://dx.doi.org/10.1016/j.chemphyslip.2013.12.004

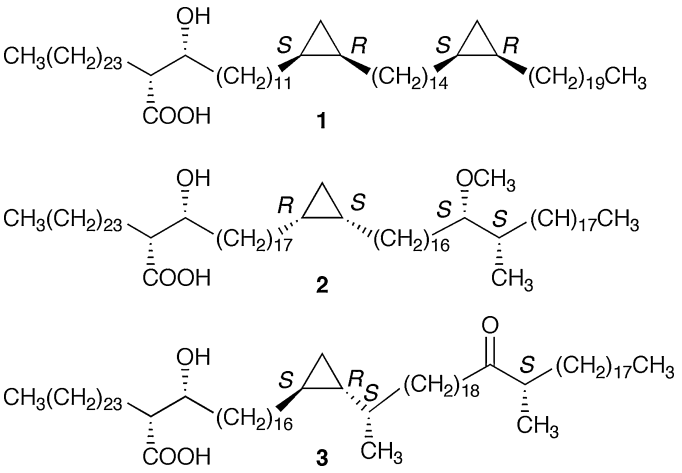

Fig. 1. Structures of the main components of the MAs from *M. tuberculosis*, α-MA **1**, methoxy-MA **2** and keto-MA **3**.

structure–function relations. Keto-MA was more prevalent when the bacteria grew in macrophages and, in the absence of keto-MA, successful entry and replication inside a macrophage-like cell-line was reduced (Yuan et al., 1998), suggesting that keto-MA plays a key role in macrophage infection. Oxygenated MAs may be essential for pathogenicity in mice (Dubnau et al., 2000) and have recently been suggested to play a major role in host lipid accumulation and foam cell formation at the site of infection and so possibly facilitate long-term persistence in the host (Peyron et al., 2008).

Additionally, natural mixtures of MAs are good antigens for serodiagnosis of TB (Pan et al., 1999; Schleicher et al., 2002), even in populations with high HIV prevalence, such as Africa (Mathebula et al., 2009; Schleicher et al., 2002; Thanyani et al., 2008). Since antibody recognition relies on macrostructural conformation, knowledge of the typically adopted structures of MA subclasses will aid in the design of serodiagnostic methods with improved specificity. With this in mind, we have examined a selection of commonly occurring MAs to establish whether their functional differences innately induce variation in MA folding.

The impact of chemical structure on the microscopic properties of MAs can be effectively visualized using molecular dynamics (MD) methods, which are suitable for handling species of this size and flexibility. In particular, atomistic MD simulation, whilst being substantially more computing intensive than, for example, coarse-grain methods typically used for membrane work (Voth, 2009), can provide atom-level information of the sort required for adequate modeling of structures with unusual functional groups, such as the cyclopropane units of MAs. This approach is also desirable as it allows stereochemistry to be explicitly addressed.

Computational studies have been done on the structure of the cell wall of *M. tuberculosis* and its permeability (Dmitriev et al., 2000; Hong and Hopfinger, 2004a,b). In these studies MAs are only represented by a generalized structure, therefore no assumptions on their individual conformations can be made. Numerous Langmuir monolayer experiments (Hasegawa et al., 2000, 2003; Villeneuve et al., 2005, 2007, 2010, 2013; Villeneuve, 2012) have shown that MA conformations change under varying lateral pressure. α-MAs tended to become fully extended, while keto-MAs stayed folded under high lateral pressure. It has been suggested that this unfolding process is influenced by the mero-functional group and the length of the carbon chains (Villeneuve et al., 2005, 2007, 2010, 2013). A principal outcome of these investigations was that most MAs can adopt a 4-chain folded conformation that can be visualized as a W-shape in two dimensions with the molecules folding at all their functional groups. These W-shapes appear to be the preferred conformations for keto-MAs, but they are less favored for α-MAs and methoxy-MAs (Villeneuve et al., 2005, 2007, 2010, 2013). Recently it has been shown that oxygenated MAs with α-methyl *trans*-cyclopropane groups fold more readily than those with *cis*-cyclopropane units (Villeneuve et al., 2013). It has also been suggested that the long MAs may need to fold into condensed conformations to be able to fit into the outer membrane of the mycobacterial cell wall (Zuber et al., 2008).

The propensity for model keto- and methoxy-MAs, from the TB-related species *Mycobacterium bovis*, to remain in a pre-set W-conformation was examined by MD (Villeneuve et al., 2007). Simulations of 20 ps MD with a restricted conformation about the hydroxyacid group were performed and then, using five points (at the ends of the chains and at functional groups) and the distances between them, it was determined either whether each MA had a preference for staying in this compact conformation or whether it unfolded. The results reinforced findings from Langmuir monolayer studies, namely that keto-MA has a preference for staying in a W-fold, while MeO-MA unfolded most of the time. They also simulated various α-MAs (Villeneuve et al., 2010) and found that α-MAs with one cyclopropane group and a double bond stayed in the W-fold longer than those α-MAs with two cyclopropane groups and that this may be due to a more energetically stable W-conformation in α-MAs containing a double bond. A relationship between chain length and unfolding was observed: more similar chain lengths between functional groups unfolded more slowly, supposedly due to a more tightly-packed W-shape. Energy level calculations of *cis*- or α-methyl *trans*-cyclopropane-containing model molecules and computer simulation studies confirmed the superior folding properties of the latter functional unit (Villeneuve et al., 2013).

Previous studies, therefore, have established that MAs from *M. tuberculosis* can articulate at all the functional group discontinuities, namely the hydroxy-acid, methoxy- and keto- units and the cyclopropane rings (Fig. 1). In particular, a fully folded "W-conformation" is very characteristic for keto-MAs, but more extended, partially-folded conformations are common in the α-MAs and methoxy-MAs. The present work aims to define a range of postulated unconstrained folds that stereochemically precise MAs from *M. tuberculosis* may adopt. The properties and possibilities of such hypothetical conformations were investigated by applying atomistic MD simulation over a significantly extended timeframe, relative to previous studies, to allow improved sampling of the potential energy surface. The results were then evaluated with principal component analysis (PCA) and self organized mapping (SOM). The folding information thus obtained illustrates clearly the importance of underlying molecular structure in directing the macromolecular 3-D conformations of representative MAs.

2. Methods

2.1. Selection of MA key reference points and working conformations

For analysis, five reference points were defined (Fig. 2) to identify the chain termini (a/e) and the specific atoms in the linking functional groups (b–d) (Villeneuve et al., 2007). Eight key distances (ab, bc, cd, de, ac, ae, ce and bd) can then be used to describe each MA fold. The distances were used in three types of analyses: principal component analysis (PCA), self organized mapping (SOM) and the identification of "W" and the alternative folds presented in Fig. 3. The idealized conformational arrangements displayed in Fig. 3 were selected to explore the properties of the various hydrocarbon chains interacting essentially in parallel. Scrutiny of these folding models shows that they can be assigned to three general types comprising "W", "U" and "Z" overall shapes, collectively

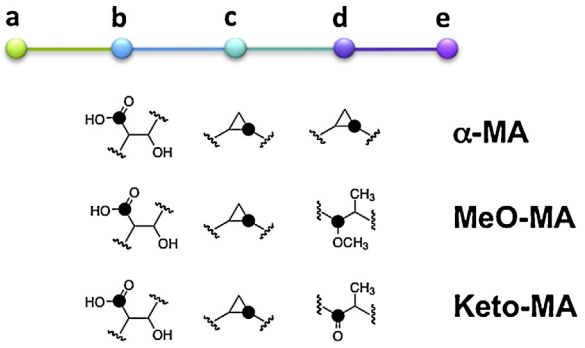

Fig. 2. Specified reference points in *M. tuberculosis* MAs drawn in the same orientation as in Fig. 1. Thus the five points indicate (a) the last carbon in the 2-alkyl chain, (b) the carbon bearing the carboxyl group, (c) the distal carbon of the proximal cyclopropane ring, (d) the carbon bearing either the keto- or the methoxy-group and the distal carbon of the distal cyclopropane ring for α-MA and (e) the end carbon of the meromycolate chain. Absolute stereochemistry is not defined.

summarized as "WUZ". Within the U-conformation category, "aU" and "eU" have "a" and "e" terminating the extended chains, respectively; "sU" is symmetrical. Similarly, "sZ" has symmetry and "aZ" and "eZ" have extended chains terminated by "a" and "e", respectively (Fig. 3).

2.2. Atomistic molecular dynamics simulations

Starting structures for the MD runs were constructed using the Accelrys Materials Studio GUI, according to the stereochemically defined structures presented in Fig. 1. These structures were prepared to represent the unfolded form of the MAs. To ensure adequate structural sampling, replicate MD runs were carried out at 298 K for each of the MAs **1**–**3** (Fig. 1) using the Compass forcefield. This forcefield was selected from those available as it provided the most consistent representation of the structural parameters of the cyclopropane groups, relative to those calculated at the semi-empirical PM3 level of theory (data not shown). Each run started from an open structure and was 4 ns in duration with 1.0 fs timesteps, sampling at 10 ps intervals to generate 400 frames. Twenty replicates were done for each MA-type. The simulations were considered to have equilibrated after 1.5 ns, at which point the pressure–potential energy plots were seen to level off (not shown). Separate analyses were performed on this portion of each run in addition to those performed on the full simulation dataset.

2.3. Principal component analysis (PCA)

PCA was used to follow the conformational changes of the molecule in the 400 frames of each simulation, frame-by-frame. GeneSight™ software (version 4.1, Biodiscovery, CA), developed for the statistical analysis of large sets of microarray data, was used to carry out PCA analyses. The distances between the structure reference points (a–e) were extracted from simulation trajectories at each frame, and used as the basis for the PCA source data.

2.4. Self organized mapping (SOM) analysis

Each of the 400 frames for each simulation were analysed by SOM using GeneSight™ software, utilising the same distance data as for the PCA. The structures were clustered onto plots with 49 groups for the full datasets and 25 groups for the equilibrated datasets, presenting a large variety of conformations (see supplementary information).

3. Results

Atomistic Molecular Dynamics simulations, whilst time intensive, offer the opportunity to explore the structural impact of atom-level molecular changes and are an ideal methodology for using with MAs, where the underlying chemical changes either affect only a small part of the molecule, or are directed through subtle changes in stereochemistry. We present the data obtained through gas phase simulation here, because this approach offers practical advantages; namely each run is reasonably fast and is able to sample a large portion of the potential surface. This rapidity and coverage is important if meaningful statistics are to be obtained from a number of replicate runs. The simulations are orders of magnitude faster than those in explicit solvent, and these systems highlight the same generalized underlying patterns resulting from the direct influence of the chemical functionality (data not shown). Being solvent free, they also provide a framework from which to understand the details of solvent effects at a later date.

3.1. Principal component analysis (PCA)

In PCA, a variance–covariance matrix is constructed in which the variability of each distance is captured, as well as its co-variation with every other distance. This array is used to identify a new variable, a vector that is a linear combination of the distances and contains the maximum amount of variance. This is the choice of the projection line or the first principal component, an eigenvector. For an $n \times n$ matrix, n eigenvectors with their corresponding eigenvalues exist. Next, the eigenvector that is orthogonal to the first, and that maximizes the remaining variability, is found. This is the second principal component.

PCA has been successfully applied to defining structural groupings within proteins (Papaleo et al., 2009; Tama et al., 2000), but its application to typical lipid structures, due to their chemical nature and smaller size is less apparent. Because mycobacterial MAs are much larger than standard lipids, with around a 60–90 carbon backbone, PCA lends itself well to the analysis of the folding of these molecules.

From the PCA results of a single representative simulation (Fig. 4) the molecular path can be followed from the open starting structures on the right-hand side to the more folded conformations on the left. Each point represents a successive frame, starting from point 1 in the top right hand side of the diagram, which represents the initial extended conformation.

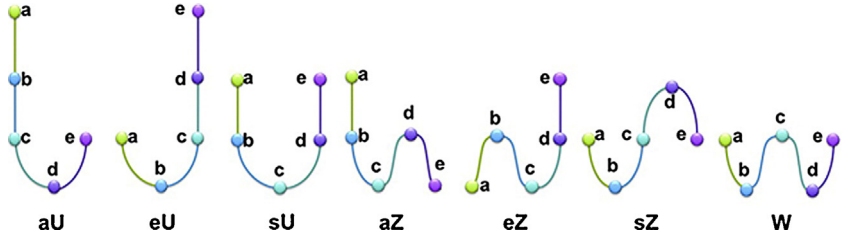

Fig. 3. Proposed mycolic acid W-, U- and Z-shaped ("WUZ") folding model conformations with interacting parallel chains.

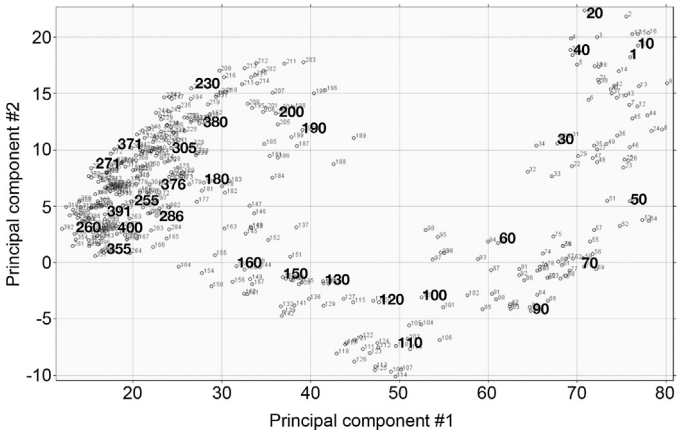

Fig. 4. A principal component analysis plot representing a single MD trajectory. Certain frame numbers have been enlarged in order to show that unfolded starting conformations occur on the right-hand side of the plot, and folded conformations that occur in later timeframes, on the left-hand side.

The results of these individual calculations were then combined for all replicates (Fig. 5a–c). From these combined PCA results with the full datasets (Fig. 5), it is seen that the extended starting conformations progressed over the course of the simulation to folded ones, primarily driven by interactions of the chains. This indicates that, *in vacuo*, the weak van der Waals interactions play a major role in directing folding, as might be expected. For MAs **1** and **2**, this folding occurred through distinct folding pathways, seen as loosely defined bands of structures between apparent clusters (Fig. 5a and b), defining low energy pathways along the potential surface between structural minima. The intensity of these bands, reflecting the population of structures on the energy surface, varied for each MA class. For MA **3**, the pattern was quite different, showing a more diffuse and less populated unfolded region (Fig. 5c). This data indicated a sampling of the potential energy surface with no apparent preferred conformational pathways and revealed that MA **3** spent less time in open conformations, demonstrating more rapid folding than observed for MAs **1** and **2** (note that the second principal co-ordinate scale is less extended than those for MAs **1** and **2**). These results predict that keto-MA has the potential to show significantly different physico-chemical, and thus biological, behavior.

3.2. Self organized mapping (SOM) analysis

To better clarify the groupings observed by PCA, SOM was utilized to generate structural clusters using an artificial neural network (Stekel, 2003; Sturn, 2000). The results could be classified into three very general types; those with a number of large distances corresponding to open forms (O), those with intermediate distances (I) and highly folded structures in which all distances between the key functional groups were very small (F). These results are summarized in Fig. 6a, and show that the bulk of structures for all three MAs were completely folded, but that significant numbers in each case were partly folded. When this analysis was carried out on the equilibrated datasets, complete folding was even more predominant (Fig. 6b). Here too, it is shown that keto-MA folded quickly since it had fewer groups of structures with open conformations.

3.3. Searching for W- and related conformations

By using the model of the W-fold (Villeneuve et al., 2005, 2007, 2010, 2013) and further considering structures whereby folding occurs specifically at the functional groups of the MAs, three general conformations, termed W, U and Z folds, can be defined

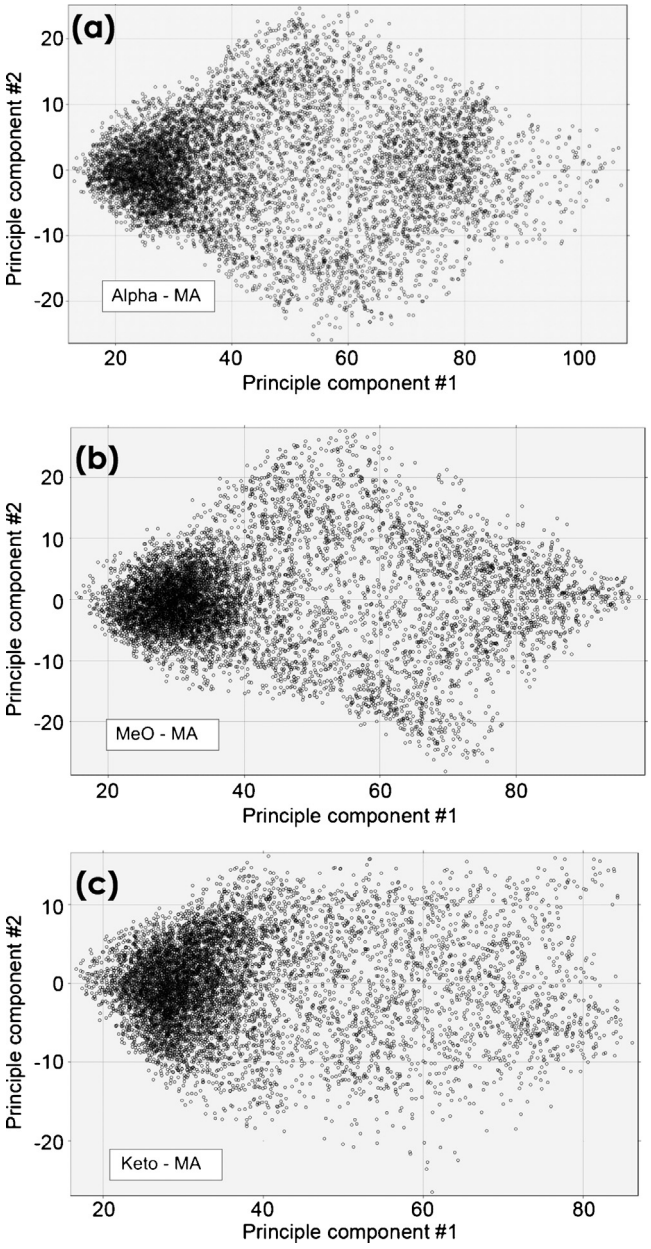

Fig. 5. Principal component analysis of combined MD trajectories for all the simulation data over the 4 ns timeframe for (a) α-; (b) methoxy- and (c) keto-MAs.

(Fig. 7). These conformations reflect the four-, two- and three-chain descriptions, respectively, found in monolayer studies (Villeneuve et al., 2005, 2007, 2010, 2013). Altogether, seven "WUZ" subsets could be assigned. Prefixes "a" (aU, aZ) and "e" (eU, eZ) are used to describe conformations when a- and e-terminated chains are unfolded, while 'symmetrical' conformations have "s" as prefix (sU, sZ).

Each frame was analysed for the seven W-, U- and Z-folds by extracting the distance data into Excel sheets with Perl scripts and analysing them with a Python script. The folds were identified according to a set of parameters described in the supplementary data (Table S1). Idealized conformers obtained from the simulations for each WUZ-fold for α-MA **1** are presented in Fig. 7. Minimization and energy calculations of selected structures from all the subclasses indicated that, on average, the lowest energy structure is the W-fold (Table S2).

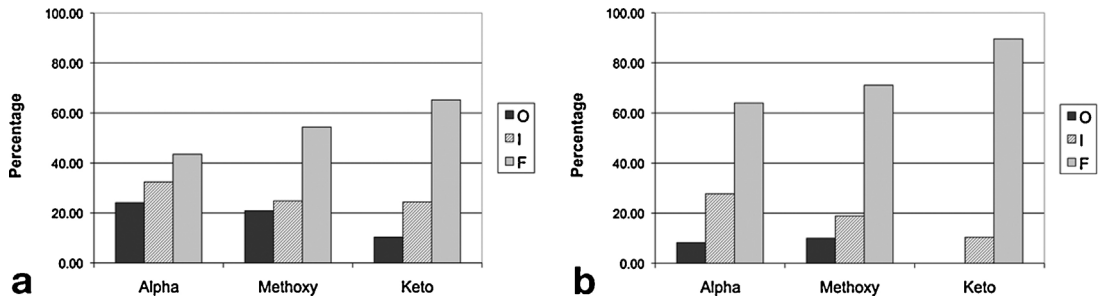

Fig. 6. Percentage of frames in open (O), intermediately folded (I) and folded (F) conformations (with ac, ae, ce and bd: ≥40 Å, >20 Å and <20 Å, respectively) for (a) full simulation data and (b) the equilibrated region.

Analysing the equilibrated datasets showed that α-MA had the highest frequency of WUZ-folds (7.93% of structures, see supplementary data, Table S3, for a detailed breakdown). The remaining MAs had lower frequencies of WUZ-folds, namely 1.35% (MeO-MA) and 3.01% (Keto-MA). The large relative difference in WUZ-fold frequencies for α-MA **1** demarcates this structure as having potentially unique properties. Thus, the difference in frequencies of specific WUZ-folds of MA, infers that the three MA structures **1**–**3** examined can be clearly differentiated based on their folding subtypes and thus that the functional group changes would have a significant impact on the macrostructure.

Comparison of WUZ-data with the SOM analysis of individual simulations showed that W, U and Z structures were separated into different SOM clusters, but it is evident that there are many more conformational groups that can still be defined. Given the lack of restrictions and external pressure applied to the simulation, and that no packing effects from additional surrounding molecules contribute, these results also demonstrate that the 2, 3 and 4-chain folds described for monolayers are both present and accessible without the restrictions imposed by membrane structure.

4. Discussion

A particular achievement of the present approach is the demonstration that the inherent structural properties of MA molecules validly predict their conformational behavior. This is particularly clear for the keto-MAs that favor W-conformations in *in vacuo* simulations but also in experimental monolayers on a Langmuir trough (Villeneuve et al., 2005, 2007, 2013). It was previously considered that the monolayer W-folding of keto-MAs might be dependent, to some extent, on hydrophilic interactions of the keto-group with the aqueous subphase but it now appears that the folding of these MAs does not necessarily depend on such interactions. Similarly,

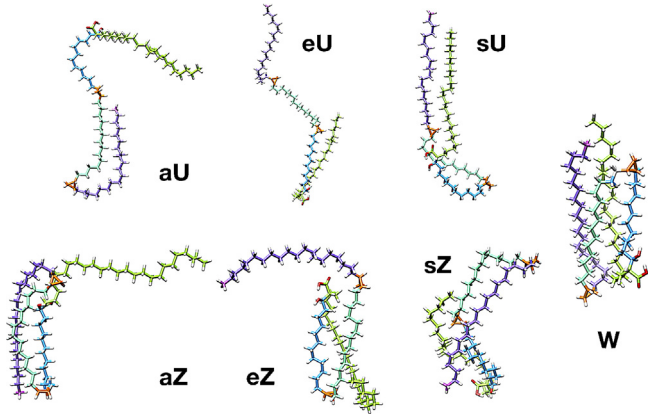

Fig. 7. Representative 'WUZ' folds for α-MA **1**. Pdb files for each structure are available as supplementary data files P1-7.

the conformational flexibility and potential versatility of *M. tuberculosis* α-MAs, demonstrated in Langmuir monolayers (Villeneuve et al., 2005, 2010), is confirmed in the present study where α-MAs were found to have the capability of accessing the widest range of stylized conformations. Again, the distinct monolayer behavior of methoxy-MAs, whose folding properties are rather intermediate between those of α-MAs and keto-MAs, is echoed by its preference for limited, but distinct, *in vacuo* folding pathways. A full understanding of the influence of the specific architecture of all mycolic acids will require extended combinations of experimental physical studies, linked with focussed calculations on individual MAs and combinations thereof. In addition to the behavior of free mycolic acids, it is important to attempt to simulate the behavior of MAs in cell envelope mycoloyl arabinogalactan and trehalose mon- and dimycolates (TDM, "cord factors"). The latter TDMs are important intermediates in the transfer of MAs into the mycobacterial cell wall (Minnikin et al., 2002) but they also have potent biological activity. Cord factors should be studied in parallel with free MAs, both in computational and physical studies, but to date only limited monolayer studies (*e.g.* Durand et al., 1979; Almog and Mannella, 1996) have been performed.

Current literature supports the notion that the balance of MA classes in mycobacteria affects biological activity, pathogenicity, virulence and cell wall permeability (Dubnau et al., 2000; Fujita et al., 2007; Glickman et al., 2000; Peyron et al., 2008; Rao et al., 2006; Yuan et al., 1998) despite what may be considered as relatively small changes in the chemical functionality. Free MAs are known to express certain features of an *M. tuberculosis* infection such as macrophage foam cell formation at the site of infection and can even cure experimental asthma in mice (Korf et al., 2006). With the advent of the total synthesis of individual MAs (Al Dulayymi et al., 2005, 2006a, 2007; Koza and Baird, 2007), it has been possible to collect data on the immune activity of different classes of MAs. Recent results distinguish specific immune activities based on the class of MA, and show specific delineation of the activities with differing oxygenated moieties and *cis versus trans*-methyl cyclopropanation (Beukes et al., 2010; Vander Beken et al., 2011). Primarily, α-MA, which shows the highest level of WUZ-conformers and also spends more time in open conformers compared to methoxy- and keto-MAs, is the least immune active. It induced no airway inflammation (Vander Beken et al., 2011) and exhibited the lowest antibody antigenicity in human TB patient sera (Beukes et al., 2010). α-MA, with no oxygenated functional group, has the greater flexibility compared to the oxygenated MAs, being the only MA that folded into all of the seven possible WUZ-folds within its full datasets. Its capability of accessing different conformations with ease was also seen by Villeneuve et al. (2007, 2010) and may be useful to modulate a changing cell wall composition in mycobacteria. Methoxy-MA showed folding *via* distinct pathways, but the lowest percentage of WUZ-folds. Methoxy-MA is the most antigenic of the three classes, with *trans*-cyclopropane stereochemistry being more antigenic than the *cis* stereochemistry

used here (Beukes et al., 2010). The *cis* isomer elicited a pronounced inflammatory response in mice, whereas the *trans* isomer partially lost this activity. Keto-MA was found to prefer more compactly folded conformations even as a single molecule, as was corroborated by monolayer packing (Villeneuve et al., 2005, 2007, 2013). Its presence in the cell wall seems key in the mycobacterial interaction with the host on entering macrophages and growing in them successfully (Yuan et al., 1998). The *trans* isomer studied here showed higher antigenicity than the *cis* isomer (Beukes et al., 2010), whereas the *cis* isomer elicited the stronger inflammatory response in mice. In contrast, the *trans* keto-MA isomer showed anti-inflammatory activity (Vander Beken et al., 2011). Oxygenated MAs have been shown to induce foam-cell formation (Korf et al., 2005), creating an environment for a dormant state of the bacteria that is rich in nutrients and possibly aids in the long-term persistence of TB infection (Peyron et al., 2008).

Although most of the mycolic acids from mycobacterial origin are covalently linked to arabinogalactan, some free mycolic acids are exported and found in mycobacterial biofilms, apparently being required for biofilm maturation in the drug-tolerant, persistent stage of the bacilli (Ojha et al., 2008). It has recently been shown that keto-MA is required in pellicle biofilm growth of *M. tuberculosis*, which is essential in conferring drug tolerance to the bacteria (Sambandan et al., 2013). Structure and conformation of free MAs may therefore be expected to be of biological significance in the development of TB in an infected patient and is an area that can be further investigated in the light of the current results. This warrants research in a better understanding of the stage specific expression of MA subtypes as such or in combination with one another.

The mycobacterial outer membrane has been visualized for the first time by cryo-electron spectroscopy (Hoffmann et al., 2008; Zuber et al., 2008). The propensity of MAs to fold at their functional groups-even in the absence of packing effects or lateral pressure-supports the model of Zuber et al. (2008) in which MAs will fold in order to fit into the 70–80 Å thick outer membrane of the cell wall. In the model that they propose for the outer membrane bilayer the MAs are folded into W-conformations, with the ends of long chains intercalating to compactly fit into the 70–80 Å outer membrane layer. The credibility of this model is supported by the results of this study, which show that all three classes of *M. tuberculosis.* MAs are able to fold into the W-conformation, the most stable conformer of the WUZ-defined folds. Within this set of data, W-folds have been found to be approximately 18–30 Å long, which will comfortably fit into one of the outer membrane leaflets. More stretched out conformations such as the Z-defined folds can also fit into this space, stretching up to approximately 40 Å. With an attachment at the acid group to arabinogalactan in the inner layer, the W and sZ-folds are most easily accommodated in this cell envelope space. The longer U-folds, reaching over 50 Å, can still be included in the overall 70–80 Å space and their extension beyond the outer membrane mid-point may be important in facilitating hydrophobic interactions with the characteristic free lipids (Minnikin et al., 2002) of *M. tuberculosis.* This study indicates that α-MAs are most likely to access U-folds and as α-MAs constitute about half of the total MAs in *M. tuberculosis*, this may be a significant factor in constituting the cell envelope in this pathogen. It is also apparent that other compact conformations that have not yet been classified, and that are consistent with these size constraints, may exist.

This preliminary study has indicated that MAs can assume a wide range of conformations when modeled as single molecules, with distinctive patterns of folding for each MA-type. Clearly detailed folding behavior needs to be explored with a greater range of mycolic acids in a systematic fashion to properly unpick the roles of each functional group in directing folding. In addition, whilst *in vacuo* calculations have provided valuable preliminary insights, especially revealing the flexibility of MAs and the same 2-, 3- and 4-chain folds proposed from monolayer studies, atomistic simulations with explicit hydration and within membrane models will no doubt reveal how more restricted environments modify the number and type of accessible conformations. Such studies may contribute towards new diagnostics and therapies against TB, which are direly needed, especially where the TB epidemic is out of control, driven by its fatal combination with HIV.

5. Conclusions

The present study is the first to explore the significance of the particular functional groups and chain lengths of the main components of the three major classes of MAs from *M. tuberculosis*, using clearly defined absolute stereochemistry (Fig. 1). These initial results from molecular dynamics simulations indicate that there are clear conformational differences between MA subclasses, which may be able to account for at least a part of the observed biological differences.

Conformations of three mycolic acid classes representative of those found in *M. tuberculosis*, simulated using atomistic MD calculations, have been statistically analysed based on eight distances between the ends of chains and functional groups. By using principal component analyses, it was shown that MAs **1**, **2** and **3** assumed folded, compact conformations from open starting structures with different folding pathways preferred for each MA. Keto-MA **3** folded most quickly. From SOM it was seen that all MAs tend towards highly folded forms with small, defined distances in these simulations. MAs spent significant periods in W, U and Z conformations that both are folded at or around the functional groups. The innate ability of MAs to fold spontaneously into WUZ-conformations, even as single molecules in vacuum, is supportive of findings from monolayer studies (Villeneuve et al., 2005, 2007, 2010, 2013; Villeneuve, 2012), where the molecules are packed tightly together under lateral pressure. α-MA adopted all the WUZ-folds most frequently. Grouping by SOM also separated W, U and Z conformations. However, from the relatively low frequencies it is evident that many other conformers, in addition to the stylized WUZ folds (Fig. 3), are both accessible and important for biological functions such as antigenic response and their conformations in the cell wall. It is clear from this study that the range of conformations, the pathways and the speed at which these conformers are accessed, are distinct for each MA subclass examined.

The value of applying a portfolio of computational methods to the exploration of the conformational possibilities of MAs has been demonstrated only for the main components of the three MA subclasses from *M. tuberculosis* (Fig. 1). However, the natural methoxy- and keto-MAs from *M. tuberculosis* include homologous series based on either *cis*- or α-methyl *trans*-cyclopropane units at the proximal position in the meromycolate chain (Minnikin, 1982; Verschoor et al., 2012). There has not been a clear understanding about why such oxygenated MAs should be comprised of two parallel series, but the recent demonstration that MA folding is facilitated by α-methyl *trans*-cyclopropane groups rather than *cis*-cyclopropane units (Villeneuve et al., 2013) has provided a partial explanation. Additional understanding of the importance of having parallel series of oxygenated MAs would be gained from the application of computational studies to a selected range of MAs, varying in chain lengths and functional group content. In particular, it would be most informative to study the developing portfolio of synthetic MAs, with known absolute stereochemistry (Al Dulayymi et al., 2003, 2005, 2006a,b, 2007; Koza and Baird, 2007; Verschoor et al., 2012) both by computational methods and direct physical approaches, such as Langmuir monolayers.

Acknowledgements

The contributions of Dr. Alexandra Simperler, Jurgens de Bruin and Mykola Rozhok, who wrote the Perl and Python scripts, and Dr. Andrew Davies, for assistance with Materials Studio, are gratefully acknowledged. Motoko Watanabe and Marion Turner contributed to the development of the 'WUZ' mycolate-folding concept, which was presented by DEM at the South African Society of Biochemistry and Molecular Biology conference in Pietermaritzburg in July 2006. This work was supported by a South African NRF grant, a travel grant from the University of Pretoria, South Africa, the Royal Society and a Commonwealth Scholarship.

Appendix A. Supplementary data

Supplementary material related to this article can be found, in the online version, at http://dx.doi.org/10.1016/j.chemphyslip.2013.12.004.

References

Al Dulayymi, J.R., Baird, M.S., Roberts, E., 2003. The synthesis of a single enantiomer of a major α-mycolic acid of *Mycobacterium tuberculosis*. J. Chem. Soc., Chem. Commun. (2), 228–229.

Al Dulayymi, J.R., Baird, M.S., Roberts, E., 2005. The synthesis of a single enantiomer of a major α-mycolic acid of *M. tuberculosis*. Tetrahedron 61, 11939–11951.

Al Dulayymi, J.R., Baird, M.S., Roberts, E., Minnikin, D.E., 2006a. The synthesis of single enantiomers of meromycolic acids from mycobacterial wax esters. Tetrahedron 62, 11867–11880.

Al Dulayymi, J.R., Baird, M.S., Mohammed, H., Roberts, E., Clegg, W., 2006b. The synthesis of one enantiomer of the α-methyl-*trans*-cyclopropane unit of mycolic acids. Tetrahedron 62, 4851–4862.

Al Dulayymi, J.R., Baird, M.S., Roberts, E., Deysel, M., Verschoor, J., 2007. The first synthesis of single enantiomers of the major methoxymycolic acid of *Mycobacterium tuberculosis*. Tetrahedron 63, 2571–2592.

Almog, R., Mannella, C.A., 1996. Molecular packing of cord factor and its interaction with phosphatidylinositol in mixed monolayers. Biophys. J. 71, 3311–3319.

Beukes, M., Lemmer, Y., Deysel, M., Al Dulayymi, J.R., Baird, M.S., Koza, G., Iglesias, M.M., Rowles, R.R., Theunissen, C., Grooten, J., Toschi, G., Roberts, V.V., Pilcher, L., Van Wyngaardt, S., Mathebula, N., Balogun, M., Stoltz, A.C., Verschoor, J.A., 2010. Structure–function relationships of the antigenicity of mycolic acids in tuberculosis patients. Chem. Phys. Lipids 163, 800–808.

Butler, W.R., Guthertz, L.S., 2001. Mycolic acid analysis by high-performance liquid chromatography for identification of *Mycobacterium* species. Clin. Microbiol. Rev. 14, 704–726.

Dmitriev, B.A., Ehlers, S., Rietschel, E.T., Brennan, P.J., 2000. Molecular mechanics of the mycobacterial cell wall: from horizontal layers to vertical scaffolds. Int. J. Med. Microbiol. 290, 251–258.

Dubnau, E., Chan, J., Raynaud, C., Mohan, V.P., Lanéelle, M.-A., Yu, K., Quémard, A., Smith, I., Daffé, M., 2000. Oxygenated mycolic acids are necessary for virulence of *Mycobacterium tuberculosis* in mice. Mol. Microbiol. 36, 630–637.

Durand, E., Welby, G., Lanéelle, G., Tocanne, J.-F., 1979. Phase behavior of cord factor and related bacterial glycolipid toxins: a monolayer study. Eur. J. Biochem. 93, 103–112.

Fujita, Y., Okamoto, Y., Uenishi, Y., Sunagawa, M., Uchiyama, T., Yano, I., 2007. Molecular and supra-molecular structure related differences in toxicity and granulomatogenic activity of mycobacterial cord factor in mice. Microb. Pathog. 43, 10–21.

Glickman, M.S., Cox, J.S., Jacobs, W.R., 2000. A novel mycolic acid cyclopropane synthetase is required for cording, persistence, and virulence of *Mycobacterium tuberculosis*. Mol. Cell 5, 717–727.

Hasegawa, T., Amino, S., Kitamura, S., Matsumoto, L., Katada, S., Nishijow, J., 2003. Study of the molecular conformation of alpha- and keto-mycolic acid monolayers by the Langmuir–Blodgett technique and Fourier transform infrared reflection-absorption spectroscopy. Langmuir 19, 105–109.

Hasegawa, T., Nishijo, J., Watanabe, M., Funayama, K., Imae, T., 2000. Conformational characterization of alpha-mycolic acid in a monolayer film by the Langmuir–Blodgett technique and atomic force microscopy. Langmuir 16, 7325–7330.

Hoffmann, C., Leis, A., Niederweis, M., Plitzko, J.M., Engelhardt, H., 2008. Disclosure of the mycobacterial outer membrane: cryo-electron tomography and vitreous sections reveal the lipid bilayer structure. Proc. Natl. Acad. Sci. U.S.A. 105, 3963–3967.

Hong, X., Hopfinger, A.J., 2004a. Construction, molecular modeling, and simulation of *Mycobacterium tuberculosis* cell walls. Biomacromolecules 5, 1052–1065.

Hong, X., Hopfinger, A.J., 2004b. Molecular modeling and simulation of *Mycobacterium tuberculosis* cell wall permeability. Biomacromolecules 5, 1066–1077.

Korf, J., Stoltz, A., Verschoor, J., De Baetselier, P., Grooten, J., 2005. The *Mycobacterium tuberculosis* cell wall component mycolic acid elicits pathogen-associated host innate immune responses. Eur. J. Immunol. 35, 890–900.

Korf, J.E., Pynaert, G., Tournoy, K., Boonefaes, T., Van Oosterhout, A., Ginneberge, D., Haegeman, A., Verschoor, J.A., De Baetselier, P., Grooten, J., 2006. Macrophage reprogramming by mycolic acid promotes a tolerogenic response in experimental asthma. Am. J. Respir. Crit. Care Med. 174, 152–160.

Koza, G., Baird, M.S., 2007. The first synthesis of single enantiomers of ketomycolic acids. Tetrahedron Lett. 48, 2165–2169.

Mathebula, N.S., Pillay, J., Toschi, G., Verschoor, J.A., Ozoemena, K.I., 2009. Recognition of anti-mycolic acid antibody at self-assembled mycolic acid antigens on a gold electrode: a potential impedimetric immunosensing platform for active tuberculosis. Chem. Commun. (23), 3345–3347.

Minnikin, D.E., Goodfellow, M., 1980. Lipid composition in the classification and identification of acid-fast bacteria. Soc. Appl. Microbiol. Symp. Ser. 8, 189–256.

Minnikin, D.E., 1982. Lipids: complex lipids, their chemistry, biosynthesis and role. In: Ratledge, C., Stanford, J. (Eds.), The Biology of Mycobacteria. Academic Press, London, UK, pp. 95–184.

Minnikin, D.E., Kremer, L., Dover, L.G., Besra, G.S., 2002. The methyl-branched fortifications of *Mycobacterium tuberculosis*. Chem. Biol. 9, 545–553.

Ojha, A.K., Baughn, A.D., Sambandan, D., Hsu, T., Trivelli, X., Guerardel, Y., Alahari, A., Kremer, L., Jacobs Jr., W.R., Hatfull, G.F., 2008. Growth of *Mycobacterium tuberculosis* biofilms containing free mycolic acids and harbouring drug-tolerant bacteria. Mol. Microbiol. 69, 164–174.

Pan, J., Fujiwara, N., Oka, S., Maekura, R., Ogura, T., Yano, I., 1999. Anti-cord factor (trehalose 6,6′-dimycolate) IgG antibody in tuberculosis patients recognizes mycolic acid subclasses. Microbiol. Immunol. 43, 863–869.

Papaleo, E., Mereghetti, P., Fantucci, P., Grandori, R., De Gioia, L., 2009. Free-energy landscape, principal component analysis, and structural clustering to identify representative conformations from molecular dynamics simulations: the myoglobin case. J. Mol. Graph. Model. 27, 889–899.

Peyron, P., Vaubourgeix, J., Poquet, Y., Levillain, F., Botanch, C., Bardou, F., Daffé, M., Emile, J.-F., Marcou, B., Cardona, P.-J., de Chastellier, C., Altare, F., 2008. Foamy macrophages from tuberculous patients' granulomas constitute a nutrient-rich reservoir for *M. tuberculosis persistance*. PLoS Pathog. 4, e1000204.

Rao, V., Gao, F., Chen, B., Jacobs, W.R., Glickman, M.S., 2006. Trans-cyclopropanation of mycolic acids on trehalose dimycolate suppresses *Mycobacterium tuberculosis* induced inflammation and virulence. J. Clin. Invest. 116, 1660–1667.

Sambandan, D., Dao, D.N., Weinrick, B.C., Vilchèze, C., Gurcha, S.S., Ojha, A., Kremer, L., Besra, G.S., Hatfull, G.F., Jacobs, W.R., 2013. Keto-mycolic acid-dependent pellicle formation confers tolerance to drug-sensitive *Mycobacterium tuberculosis*. MBio 4, e00222–e313.

Schleicher, G.K., Feldman, C., Vermaak, Y., Verschoor, J.A., 2002. Prevalence of anti-mycolic acid antibodies in patients with pulmonary tuberculosis co-infected with HIV. Clin. Chem. Lab. Med. 40, 882–887.

Song, S.H., Park, K.U., Lee, J.H., Kim, E.C., Kim, J.Q., Song, J., 2009. Electrospray ionization-tandem mass spectrometry analysis of the mycolic acid profiles for the identification of common clinical isolates of mycobacterial species. J. Microbiol. Methods 77, 165–177.

Stekel, D., 2003. Analysis of relationships between genes, tissues of treatments. In: Stekel, D. (Ed.), Microarray Bioinformatics. , 1st ed. Cambridge University Press, Cambridge, United Kingdom, pp. 151–180.

Sturn, A., 2000. Cluster analysis for large scale gene expression studies. In: Biomedical Engineering. Institute for Biomedical Engineering, Graz University of Technology/Institute for Genomic Research, Graz, Austria/Rockville, MD, USA, pp. 28–58.

Tama, F., Miyashita, O., Kitao, A., Go, N., 2000. Molecular dynamics simulation shows large volume fluctuations of proteins. Eur. Biophys. J. 29, 472–480.

Thanyani, S.T., Roberts, V., Siko, D.G., Vrey, P., Verschoor, J.A., 2008. A novel application of affinity biosensor technology to detect antibodies to mycolic acid in tuberculosis patients. J. Immunol. Methods 332, 61–72.

Vander Beken, S., Al Dulayymi, J.R., Naessens, T., Koza, G., Maza-Iglesias, M., Rowles, R., Theunissen, C., De Medts, J., Lanckacker, E., Baird, M.S., Grooten, J., 2011. Molecular structure of the *Mycobacterium tuberculosis* virulence factor, mycolic acid, determines the elicited inflammatory pattern. Eur. J. Immunol. 41, 450–460.

Verschoor, J.A., Baird, M.S., Grooten, J., 2012. Towards understanding the functional diversity of cell wall mycolic acids of *Mycobacterium tuberculosis*. Prog. Lipid Res. 51, 325–339.

Villeneuve, M., Kawai, M., Kanashima, H., Watanabe, M., Minnikin, D.E., Nakahara, H., 2005. Temperature dependence of the Langmuir monolayer packing of mycolic acids from *Mycobacterium tuberculosis*. Biochim. Biophys. Acta Biomembr. 1715, 71–80.

Villeneuve, M., Kawai, M., Watanabe, M., Aoyagi, Y., Hitotsuyanagi, Y., Takeya, K., Gouda, H., Hirono, S., Minnikin, D.E., Nakahara, H., 2007. Conformational behavior of oxygenated mycobacterial mycolic acids from *Mycobacterium bovis* BCG. Biochim. Biophys. Acta Biomembr. 1768, 1717–1726.

Villeneuve, M., Kawai, M., Watanabe, M., Aoyagi, Y., Hitotsuyanagi, Y., Takeya, K., Gouda, H., Hirono, S., Minnikin, D.E., Nakahara, H., 2010. Differential conformational behaviors of alpha-mycolic acids in Langmuir monolayers and computer simulations. Chem. Phys. Lipids 163, 569–579.

Villeneuve, M., Kawai, M., Horiuchi, K., Watanabe, M., Aoyagi, Y., Hitotsuyanagi, Y., Takeya, K., Gouda, H., Hirono, S., Minnikin, D.E., 2013. Conformational folding of mycobacterial methoxy and ketomycolic acids facilitated by α-methyl trans-cyclopropane groups rather than cis-cyclopropane units. Microbiology 159, 2405–2415.

Villeneuve, M., 2012. Characteristic conformational behaviors of representative mycolic acids in the interfacial monolayer. In: Cardona, P.-J. (Ed.), Understanding Tuberculosis-Deciphering the Secret Life of the *Bacilli*. InTech – Open Access Publisher, Rijeka, Croatia, pp. 317–334, ISBN-13: 978-953-307-946-2 http://www.intechopen.com/books/understanding-tuberculosis-deciphering-the-secret-life-of-the-bacilli

Voth, G.A., 2009. Coarse-Graining of Condensed Phase and Biomolecular Systems. CRC Press, Taylor & Francis Group, Boca Raton, FL.

Watanabe, M., Aoyagi, Y., Ridell, M., Minnikin, D.E., 2001. Separation and characterization of individual mycolic acids in representative mycobacteria. Microbiology 147, 1825–1837.

Watanabe, M., Aoyagi, Y., Mitome, H., Fujita, T., Naoki, H., Ridell, M., Minnikin, D.E., 2002. Location of functional groups in mycobacterial meromycolate chains; the recognition of new structural principles in mycolic acids. Microbiology 148, 1881–1902.

Yuan, Y., Zhu, Y., Crane, D.D., Barry, C.E., 1998. The effect of oxygenated mycolic acid composition on cell wall function and macrophage growth in *Mycobacterium tuberculosis*. Mol. Microbiol. 29, 1449–1458.

Zuber, B., Chami, M., Houssin, C., Dubochet, J., Griffiths, G., Daffé, M., 2008. Direct visualization of the outer membrane of mycobacteria and corynebacteria in their native state. J. Bacteriol. 190, 5672–5680.